Magnetoinfrared Spectroscopy of Landau Levels and Zeeman Splitting of Three-Dimensional Massless Dirac Fermions in $ZrTe_5$

R. Y. Chen,[1] Z. G. Chen,[2] X.-Y. Song,[1] J. A. Schneeloch,[3] G. D. Gu,[3] F. Wang,[1,4,*] and N. L. Wang[1,4,†]
[1]International Center for Quantum Materials, School of Physics, Peking University, Beijing 100871, China
[2]National High Magnetic Field Laboratory, Tallahassee, Florida 32310, USA
[3]Condensed Matter Physics and Materials Science Department, Brookhaven National Lab, Upton, New York 11973, USA
[4]Collaborative Innovation Center of Quantum Matter, Beijing, China
(Received 26 August 2015; published 22 October 2015)

We present a magnetoinfrared spectroscopy study on a newly identified three-dimensional (3D) Dirac semimetal $ZrTe_5$. We observe clear transitions between Landau levels and their further splitting under a magnetic field. Both the sequence of transitions and their field dependence follow quantitatively the relation expected for 3D *massless* Dirac fermions. The measurement also reveals an exceptionally low magnetic field needed to drive the compound into its quantum limit, demonstrating that $ZrTe_5$ is an extremely clean system and ideal platform for studying 3D Dirac fermions. The splitting of the Landau levels provides direct, bulk spectroscopic evidence that a relatively weak magnetic field can produce a sizable Zeeman effect on the 3D Dirac fermions, which lifts the spin degeneracy of Landau levels. Our analysis indicates that the compound evolves from a Dirac semimetal into a topological line-node semimetal under the current magnetic field configuration.

DOI: 10.1103/PhysRevLett.115.176404 PACS numbers: 71.55.Ak, 71.70.Di, 78.20.-e

3D topological Dirac or Weyl semimetals are new kinds of topological materials that possess linear band dispersion in the bulk along all three momentum directions [1–7]. Their low-energy quasiparticles are the condensed matter realization of Dirac and Weyl fermions in relativistic high energy physics [8,9]. These materials are expected to host many unusual phenomena [10–12], in particular the chiral and axial anomaly associated with Weyl fermions [3,13–15]. It is well known that the Dirac nodes are protected by both time-reversal and space inversion symmetry. Since a magnetic field breaks time-reversal symmetry, a Dirac node may be split into a pair of Weyl nodes along the magnetic field direction in the momentum space [16–18] or transformed into line nodes [17,19]. Therefore, a Dirac semimetal can be considered as a parent compound to realize other topological variant quantum states. However, past 3D Dirac semimetal materials (e.g., Cd_3As_2) suffer from the problem of large residual carrier density, which requires very high magnetic field (e.g., above 60 T) to drive them to their quantum limit [20,21]. This makes it extremely difficult to explore the transformation from Dirac to Weyl or line-node semimetals. Up to now there is no direct evidence of such transformations.

$ZrTe_5$ appears to be a new topological 3D Dirac material that exhibits novel and interesting properties. The compound crystallizes in the layered orthorhombic crystal structure, with prismatic $ZrTe_6$ chains running along the crystallographic a axis and linked along the c axis via zigzag chains of Te atoms to form two-dimensional (2D) layers. Those layers stack along the b axis. A recent *ab initio* calculation suggests that bulk $ZrTe_5$ locates close to the phase boundary between weak and strong topological insulators [22]. However, more recent transport and ARPES experiments identify it to be a 3D Dirac semimetal with only one Dirac node at the Γ point [23]. Interestingly, a chiral magnetic effect associated with the transformation from a Dirac to Weyl semimetal was observed on $ZrTe_5$ through a magnetotransport measurement [23]. Our recent optical spectroscopy measurement at zero field revealed clearly a linear energy dependence of optical conductivity as another hallmark of 3D massless Dirac fermions [24].

In this Letter, we present a magnetoinfrared spectroscopy study on $ZrTe_5$ single crystals. We observe clear transitions between Landau levels and their further splitting under magnetic field. Both the sequence of transitions and their field dependence follow quantitatively the relation expected for 3D *massless* Dirac fermions. Furthermore, the measurement reveals an exceptionally low magnetic field (about 1 T) needed to drive the compound into its quantum limit. Both facts demonstrate that $ZrTe_5$ is an extremely clean system and ideal platform for studying 3D Dirac fermions. The presence of further splitting of Landau levels, which has never been observed in 2D massless Dirac fermions, e.g., graphene, provides direct evidence for the lifting of spin degeneracy of Landau levels, an effect being linked to the transformation from a Dirac semimetal to a line node or Weyl semimetal. Our theoretical analysis indicates that the former one is more likely realized in the present magnetic field configuration.

Figure 1 shows the reflectance spectra under different magnetic field $R(B)$ renormalized by the zero field reflectance $R(0)$ in the far- and midinfrared region. For the

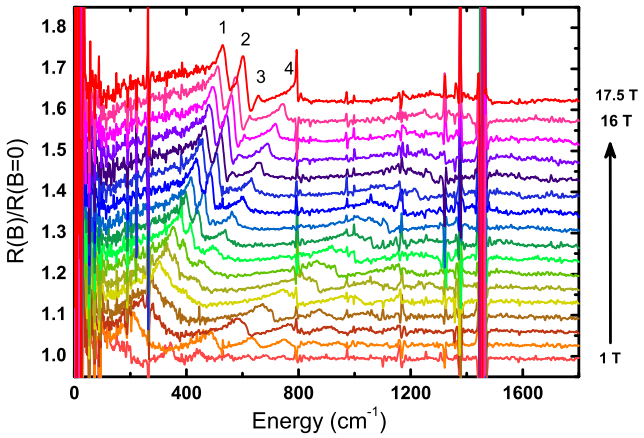

FIG. 1 (color online). The relative reflectivity of $ZrTe_5$ under magnetic field, as a function of energy. The spectra are shifted upward by equal intervals corresponding to different B.

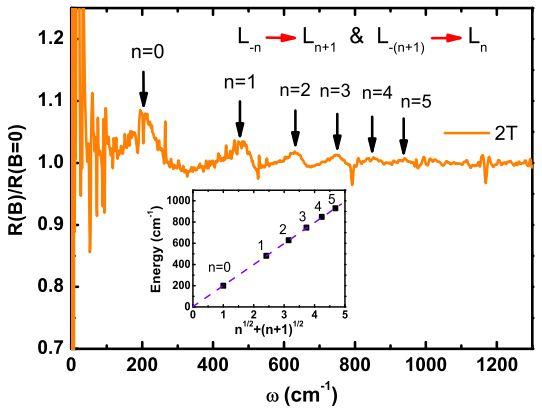

FIG. 2 (color online). The wave number dependent relative reflectivity $R(B)/R(0)$ under magnetic field of 2 T. $n = 0\ldots5$ point to six different peaks in sequence. The inset shows the linear dependence of the transition energies between Landau levels on $\sqrt{n} + \sqrt{n+1}$. The dashed line is a guide to the eyes.

lowest magnetic field (1 T), a series of peaks could be clearly resolved, which keep growing more pronounced and shift to higher energies when the field strength B increases. In optical reflectance measurement, such peak features usually come from the interband transitions. Since these sharp peaks emerge in the reflectivity only by applying magnetic field, it is natural to connect them to the Landau quantization of 3D Dirac electrons. Thus, the peaks should stem from electronic transitions connecting different Landau levels. Significantly, the first broad peak, which appears at the lowest energy, gradually split into four narrow peaks as B increases. This character is quite intriguing and has never been observed before, which will be explained in detail later. For the sake of convenience, they are marked by the numbers 1, 2, 3, 4, respectively, at the top of Fig. 1. However, the splittings of other peaks located at higher energies are rather vague in this plot.

In order to verify our speculation on the origin of the emerging peaks and capture the underlying physics of a 3D Dirac semimetal, we examine the sequence of peaks observed at low field. For a 3D system, the band structure would transform into a set of 1D Landau levels by applying strong enough magnetic field, which are only dispersive along the field direction. Theoretical calculation on an isolated Weyl point has suggested that the magneto-optical conductivity is constituted of a series of asymmetric peaks lying on top of a linear background [25,26]. Especially, the peaks associated with the allowed interband transitions in the Landau level structure occur at $\omega \propto \sqrt{n} + \sqrt{n+1}$, corresponding to transition from L_{-n} to L_{n+1} or from $L_{-(n+1)}$ to L_n, where L_n represents for the nth Landau level. This conclusion applies to the 3D massless Dirac fermion as well, because the massless Dirac fermion can be thought as two sets of Weyl fermions with opposite chirality.

A linear rising optical conductivity has been revealed in our previous zero field spectroscopic experiment on $ZrTe_5$ single crystals [24], which already provides strong evidence for 3D massless Dirac or Weyl femions. We enlarged the results of $B = 2$ T as displayed in Fig. 2, in which six peaks could be clearly resolved. The positions of these peaks are identified to be about 202, 480, 628, 748, 856, and 937 cm^{-1} in sequence. The energy ratios of the peaks observed here can be approximately reduced to 1: $1+\sqrt{2}$: $\sqrt{2}+\sqrt{3}$: $\sqrt{3}+\sqrt{4}$: $\sqrt{4}+\sqrt{5}$: $\sqrt{5}+\sqrt{6}$, in nearly perfect accordance with the predicted massless Dirac semimetal behavior. This results in a linear dependence of the transition energy between Landau levels on $\sqrt{n} + \sqrt{n+1}$, as shown in the inset of the figure. From this observation, the first peak can be unambiguously determined to correspond to $n = 0$, ascribed to transitions from L_0 to L_1 and L_{-1} to L_0. Only when the chemical potential lies in between L_1 and L_{-1}, can this transition be clearly visible [26]. This is quite exciting because it demonstrates that the quantum limit could be easily approached by magnetic field as low as 1 T, where the $n = 0$ peak is distinctively observed. As a contrast, the quantum limit of the well-known Dirac semimetal Cd_3As_2 cannot be reached with magnetic field lower than 65 T [20,21]. It indicates that the $ZrTe_5$ compound is extremely close to an ideal Dirac semimetal, with the chemical potential lying in the vicinity of the Dirac point, and meanwhile it is an extraordinarily clean system. We anticipate that our finding of easy access of the quantum limit will motivate many other experimental probes on this compound. In the Supplemental Material [27] we perform a more detailed analysis of this peak sequence and obtain estimates of the average ac-plane Fermi velocity $v_\perp = \sqrt{v_a v_c} \sim 4.84 \times 10^5$ (m/s) and a vanishingly small Dirac mass $|m| \sim 2$ (cm^{-1}).

In Fig. 1, where $R(B)/R(0)$ was shifted by equal interval with regard to increasing magnetic field, it is noted that the peak positions evolve in a way much like the parabolic

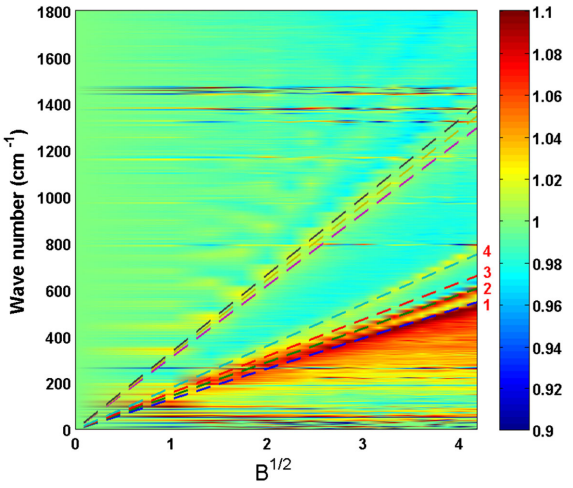

FIG. 3 (color online). The pseudocolor photograph of the relative reflectivity $R(B)/R(0)$ as functions of wave number and $\sqrt{B}$. The dashed lines are linear fittings of the peak energies dependent on $\sqrt{B}$.

fashion as B. To further illustrate the characteristic features of the Landau levels, we plot $R(B)/R(0)$ in a pseudo-color photograph as a function of $\sqrt{B}$. It is clearly seen in Fig. 3 that the wave numbers of the peaks are basically linear proportional to $\sqrt{B}$. The dashed lines are guides for the eye, whose intercepts at 0 T are all absolute zero. For a single massless 3D Dirac node, the nth Landau levels caused by magnetic field are dispersive only along the field direction (see Supplemental Material [27] for more details), with doubly degenerate $n \neq 0$ levels $E_n(k_\parallel) = \mathrm{sgn}(n)\sqrt{2v_\perp^2 eB\hbar|n| + \hbar^2 v_\parallel^2 k_\parallel^2}$, and $E_0(k_\parallel) = \pm\hbar v_\parallel k_\parallel$ for $n = 0$. If we neglect the dispersion along the magnetic field direction, then $E_n \propto \sqrt{B}$. As a comparison, for free electron systems, the magnetic induced Landau level obeys $E_n = (n + \frac{1}{2})\hbar\omega_c$, where ω_c is the the cyclotron angular velocity and proportional to B instead of $\sqrt{B}$. Additionally, the Landau level energy of massive 3D Dirac fermions in topological insulator Bi_2Se_3 is reported to be in linear scale with B as well [28]. Therefore, the $\sqrt{B}$ dependence in Fig. 3 intensively implies again the characteristic property of 3D massless Dirac fermions in $ZrTe_5$ under magnetic field.

In addition to the sequence of peaks at low field, the peak splitting shown in Fig. 1 could also be well resolved in Fig. 3. The $n = 0$ peak evolves into four peaks at high magnetic field, with two very pronounced ones at lower energies and two relatively weak ones at higher energies. They are labeled as "1, 2, 3, 4", respectively, in accordance with Fig. 1 The splittings of the rest of the peaks are, although too vague to be precisely identified, certain to exist. The $n = 1$ peak, arising from transitions from L_{-2} to L_1 and L_{-1} to L_2, seems to split into 3 peaks. Such splitting has never been observed in a 2D massless Dirac fermion system, for example, graphene [29].

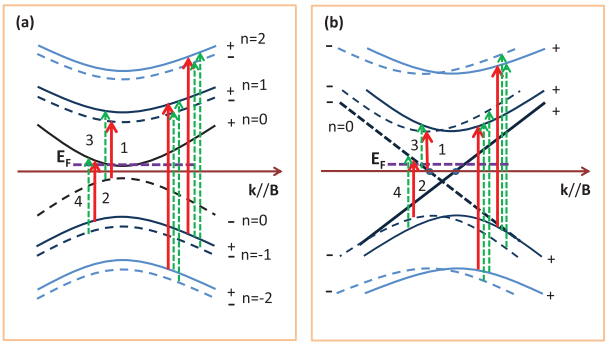

FIG. 4 (color online). Two proposed scenarios. The left panel (a) shows the splitting of Landau levels simply caused by the Zeeman effect. The strong spin-orbit coupling could lead to a mixing of spin-up and spin-down components. So the split + (solid lines) and—(dashed lines) levels do not have pure spin-up and spin-down components. This would allow inter-Landau level transitions to occur with opposite signs, however, weak in intensity. The purple dashed line is the Fermi energy E_F. A Zeeman field without orbital effect will transform 3D Dirac node into line nodes in this case [17]. The right panel (b) represents the Landau levels of a Weyl semimetal induced by the magnetic field. The crossing points of $n = 0$ Landau levels with the horizontal axis are the would-be Weyl points, if the orbital effect of the magnetic field is ignored. The solid lines and dashed lines represent the two sets of Landau levels from the two Weyl nodes with opposite chirality. Transitions between Landau levels of opposite chirality will have weaker intensity. In both panels, the red solid arrows represent transitions between Landau levels of the same spin or chirality, whereas the green dashed arrows indicate different spin or chirality.

We now explore the underlying mechanism for the splitting. We will show that this splitting can be naturally explained by the Zeeman effects of magnetic field on 3D Dirac fermions. The effect of the Zeeman field on Dirac semimetals has been thoroughly studied by Burkov *et al.* [17]. It was pointed out that the Zeeman field may split the Dirac node into two Weyl nodes, or transform the Dirac node into "line nodes" [17]. Further including the orbital effects of the magnetic field will generate Zeeman-split Landau levels, schematically shown in Fig. 4. Here we will briefly explain the two possible scenarios and leave the details in the Supplemental Material [27].

The first scenario we consider is the line-nodes picture, with the resulting Landau level structure depicted in Fig. 4(a). The doubly degenerate Landau levels $E_n(k_\parallel)$ for $n \neq 0$ from 3D Dirac fermions will be split into $E_{n,\pm} \sim E_n(k_\parallel) \pm \bar{g}\mu_B B/2$, where $\bar{g}$ is the average Landé g factor for the conduction and valence bands of 3D Dirac fermions. The $n = 0$ Landau levels $E_0(k_\parallel) = \pm\hbar v_\parallel k_\parallel$ will mix around $k_\parallel = 0$ and open a gap of size $\bar{g}\mu_B B$ there, and become $E_{0,\pm} \sim \pm\sqrt{\hbar^2 v_\parallel^2 k_\parallel^2 + (\bar{g}\mu_B B/2)^2}$. The split Landau levels are labeled by "spin" indices "+" and "−" in Fig. 4(a), which indicate that the states are spin-up or

spin-down at $k_\parallel = 0$. However, with $k_\parallel \neq 0$ the split Landau levels are not purely spin-up or spin-down due to strong spin-orbit coupling. Optical transitions between levels of the same spin indices can happen at $k_\parallel = 0$, and produce strong peaks in optical conductivity (thus reflectivity) [26], but transitions between levels of opposite spin indices will be suppressed at $k_\parallel = 0$, leading to weak and broad peaks. Therefore the original $n = 0$ peak will split into two strong peaks—1 from $L_{0,-}$ to $L_{1,-}$, and 2 from $L_{-1,+}$ to $L_{0,+}$, and two weak peaks—3 from $L_{0,-}$ to $L_{1,+}$, and 4 from $L_{-1,-}$ to $L_{0,+}$. Peaks 1 and 2 can have different energy if the chemical potential is not in the gap between $L_{0,-}$ and $L_{0,+}$ as depicted in Fig. 4(a), or if the conduction and valence bands of 3D Dirac fermion have different g factor (see Supplemental Material [27]). In any case, the splitting between peak 3 and peak 1, and between peak 4 and peak 2 will be about $\bar{g}\mu_B B$. Based on previous *ab initio* results [22] on $ZrTe_5$ and the experimental setup, we conclude that this scenario is the most likely explanation of our observation (see Supplemental Material [27] for details).

The second and more interesting scenario is the "Weyl nodes" picture illustrated in Fig. 4(b). In this case the Zeeman field effectively shifts the wave vector parallel to field by $\pm\bar{g}\mu_B B/2\hbar v_\parallel$, where the $\pm$ sign depends on the chirality of the Weyl fermions. The degenerate $n \neq 0$ Landau levels become $E_{n,\pm}(k_\parallel) \sim E_n(k_\parallel \mp \bar{g}\mu_B B/2\hbar v_\parallel)$, and the $n = 0$ Landau levels become $E_{0,\pm}(k_\parallel) \sim \pm\hbar v_\parallel k_\parallel - \bar{g}\mu_B B/2$. In this scenario transitions between Landau levels of the same (different) chirality will have strong (weak) intensity. The original $n = 0$ peak will also split into two strong peaks—1from $L_{0,-s}$ to $L_{1,-s}$, and 2 from $L_{-1,-s}$ to $L_{0,-s}$, and two weak peaks—3 from $L_{0,-s}$ to $L_{1,s}$, and 4 from $L_{-1,s}$ to $L_{0,-s}$, where $s = \pm$. Peak 1 and 2 can have different energy if the chemical potential is not at the charge neutrality as depicted in Fig. 4(b). However, the splitting between peaks 3 and 1 will, in general, not be linear in B, unless the conduction and valence bands have very different g factors. According to our analysis [27], this scenario is more likely to happen when the field is applied along the crystal c direction.

From the peak positions of 1, 2, 3, and 4 we can immediately obtain the dependence of the split energy as a function of the magnetic field. Figure 5 displays the magnetic field dependence of $E_4 - E_2$ above 6 T and $E_3 - E_1$ above 13 T, respectively. The energy positions for peak 3 could not be well resolved below 12 T, so the energy difference of $E_3 - E_1$ is plotted only at high magnetic field. Obviously, both $E_4 - E_2$ and $E_3 - E_1$ exhibit good linear dependence, in better agreement with the first line-nodes scenario. The energy splitting is roughly 10.5 cm^{-1}/T(~1.3 meV/T) for $E_4 - E_2$ and 7.4 cm^{-1}/T(~0.92 meV/T) for $E_3 - E_1$. According to previous discussions, this leads to estimates of the average

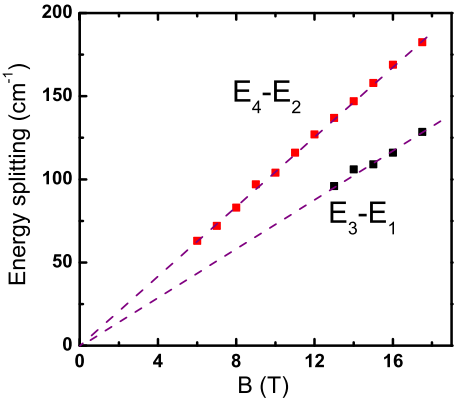

FIG. 5 (color online). The magnetic field dependent energy difference of $E_3 - E_1$ and $E_4 - E_2$. They represent the Landau level splittings for the conduction and valence bands, respectively.

g factor being 22.5 or 15.8, from the $E_4 - E_2$ or $E_3 - E_1$ splittings, respectively.

It was known that the g factor reaches about 37 for Cd_3As_2 [30], which is even bigger than our estimated g factor for the $ZrTe_5$ compound. We do not yet have a good explanation for the discrepancy between $E_4 - E_2$ and $E_3 - E_1$ splittings. Based on our analysis in the Supplemental Material [27], this could be due to the broad nature of the weaker peaks, and the current analysis may overestimate the g factors for this reason.

The transitions associated with $L_{-2} \to L_1$ and $L_{-1} \to L_2$ are much more complex. Analogous to the transitions between L_0 and $L_{\pm 1}$, the selection rule permissive ones (indicated by the red solid arrows in Fig. 4) should be more pronounced than those between opposite spin orientations (dashed green arrows). Considering possible different splittings of the valence and conduction bands, the $n = 1$ peak appeared in $R(B)/R(0)$ is supposed to contain at least three components.

In summary, by performing magneto-optical measurement on the single crystalline 3D massless Dirac semimetal $ZrTe_5$, we have clearly observed the magnetic field induced Landau levels, evidenced by regular organized peaks shown in the renormalized reflectivity $R(B)/R(0)$. Particularly, the first peak is identified to originate from the transitions between the zeroth and first Landau levels, which reveals the Fermi energy lies very close to the Dirac point. The appearance of the first peak under magnetic field as low as 1 T demonstrates an exceptionally low quantum limit of $ZrTe_5$ compared to other 3D Dirac semimetals, which provided an elegant platform to explore more intriguing nontrivial quantum phenomena. Of most importance, the fourfold splitting of the first peak yields direct and clear evidence for the release of spin degeneracy of the Landau level, hence the transformation from a Dirac semimetal into line-node or Weyl semimetal. Our theoretical modeling and analysis indicate that the former one is

more likely realized in the present magnetic field configuration.

We acknowledge very helpful discussions with Z. Fang, H. M. Weng, X. C. Xie, D. H. Lee, L. Fu, Q. Li, X. Dai, and H. W. Liu. This work was supported by the National Science Foundation of China (Grants No. 11120101003, No. 11327806, No. 11374018), and the 973 project of the Ministry of Science and Technology of China (Grants No. 2011CB921701, No. 2012CB821403, No. 2014CB920902). Work at Brookhaven is supported by the Office of Basic Energy Sciences, Division of Materials Sciences and Engineering, U.S. Department of Energy under Contract No. DE-SC00112704.

R. Y. C. and Z. G. C. contributed equally to this work.

*wangfa@pku.edu.cn
†nlwang@pku.edu.cn

[1] Z. Wang, Y. Sun, X.-Q. Chen, C. Franchini, G. Xu, H. Weng, X. Dai, and Z. Fang, Phys. Rev. B **85**, 195320 (2012).
[2] Z. Wang, H. Weng, Q. Wu, X. Dai, and Z. Fang, Phys. Rev. B **88**, 125427 (2013).
[3] X. Wan, A. M. Turner, A. Vishwanath, and S. Y. Savrasov, Phys. Rev. B **83**, 205101 (2011).
[4] Z. K. Liu, B. Zhou, Y. Zhang, Z. J. Wang, H. M. Weng, D. Prabhakaran, S.-K. Mo, Z. X. Shen, Z. Fang, X. Dai *et al.*, Science **343**, 864 (2014).
[5] Z. K. Liu, J. Jiang, B. Zhou, Z. J. Wang, Y. Zhang, H. M. Weng, D. Prabhakaran, S.-K. Mo, H. Peng, P. Dudin *et al.*, Nat. Mater. **13**, 677 (2014).
[6] S. Borisenko, Q. Gibson, D. Evtushinsky, V. Zabolotnyy, B. Büchner, and R. J. Cava, Phys. Rev. Lett. **113**, 027603 (2014).
[7] M. Neupane, S.-Y. Xu, R. Sankar, N. Alidoust, G. Bian, C. Liu, I. Belopolski, T.-R. Chang, H.-T. Jeng, H. Lin *et al.*, Nat. Commun. **5**, 3786 (2014).
[8] S. M. Young, S. Zaheer, J. C. Y. Teo, C. L. Kane, E. J. Mele, and A. M. Rappe, Phys. Rev. Lett. **108**, 140405 (2012).
[9] D. E. Kharzeev, Prog. Part. Nucl. Phys. **75**, 133 (2014).
[10] L. P. He, X. C. Hong, J. K. Dong, J. Pan, Z. Zhang, J. Zhang, and S. Y. Li, Phys. Rev. Lett. **113**, 246402 (2014).
[11] T. Liang, Q. Gibson, M. N. Ali, M. Liu, R. J. Cava, and N. P. Ong, Nat. Mater. **14**, 280 (2015).
[12] S.-Y. Xu, C. Liu, S. K. Kushwaha, R. Sankar, J. W. Krizan, I. Belopolski, M. Neupane, G. Bian, N. Alidoust, T.-R. Chang *et al.*, Science **347**, 294 (2015).
[13] Y. Chen, S. Wu, and A. A. Burkov, Phys. Rev. B **88**, 125105 (2013).
[14] P. Hosur and X.-L. Qi, Phys. Rev. B **91**, 081106 (2015).
[15] A. C. Potter, I. Kimchi, and A. Vishwanath, Nat. Commun. **5**, 5161 (2014).
[16] A. A. Burkov and L. Balents, Phys. Rev. Lett. **107**, 127205 (2011).
[17] A. A. Burkov, M. D. Hook, and L. Balents, Phys. Rev. B **84**, 235126 (2011).
[18] E. V. Gorbar, V. A. Miransky, and I. A. Shovkovy, Phys. Rev. B **88**, 165105 (2013).
[19] M. Phillips and V. Aji, Phys. Rev. B **90**, 115111 (2014).
[20] A. Narayanan, M. D. Watson, S. F. Blake, N. Bruyant, L. Drigo, Y. L. Chen, D. Prabhakaran, B. Yan, C. Felser, T. Kong *et al.*, Phys. Rev. Lett. **114**, 117201 (2015).
[21] J. Cao, S. Liang, C. Zhang, Y. Liu, J. Huang, Z. Jin, Z.-G. Chen, Z. Wang, Q. Wang, J. Zhao *et al.*, Nat. Commun. **6**, 7779 (2015).
[22] H. Weng, X. Dai, and Z. Fang, Phys. Rev. X **4**, 011002 (2014).
[23] Q. Li, D. E. Kharzeev, C. Zhang, Y. Huang, I. Pletikosic, A. V. Fedorov, R. D. Zhong, J. A. Schneeloch, G. D. Gu, and T. Valla, arXiv:1412.6543.
[24] R. Y. Chen, S. J. Zhang, J. A. Schneeloch, C. Zhang, Q. Li, G. D. Gu, and N. L. Wang, Phys. Rev. B **92**, 075107 (2015).
[25] P. Hosur, S. A. Parameswaran, and A. Vishwanath, Phys. Rev. Lett. **108**, 046602 (2012).
[26] P. E. C. Ashby and J. P. Carbotte, Phys. Rev. B **87**, 245131 (2013).
[27] See Supplemental Material at http://link.aps.org/supplemental/10.1103/PhysRevLett.115.176404 for experimental details, theoretical modeling and calculations.
[28] M. Orlita, B. A. Piot, G. Martinez, N. K. S. Kumar, C. Faugeras, M. Potemski, C. Michel, E. M. Hankiewicz, T. Brauner, i. c. v. Drašar *et al.*, Phys. Rev. Lett. **114**, 186401 (2015).
[29] M. L. Sadowski, G. Martinez, M. Potemski, C. Berger, and W. A. de Heer, Phys. Rev. Lett. **97**, 266405 (2006).
[30] S. Jeon, B. B. Zhou, A. Gyenis, B. E. Feldman, I. Kimchi, A. C. Potter, Q. D. Gibson, R. J. Cava, A. Vishwanath, and A. Yazdani, Nat. Mater. **13**, 851 (2014).